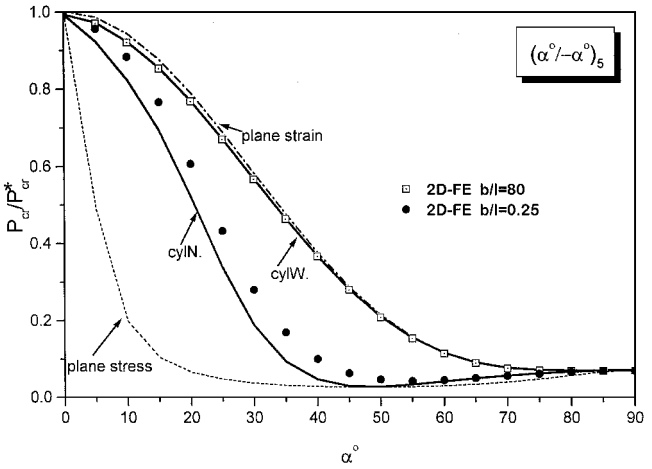

Fig. 3 Buckling load vs orientation angle of $(\alpha/-\alpha)_5$ laminate for different constitutive models compared to two-dimensional plate results.

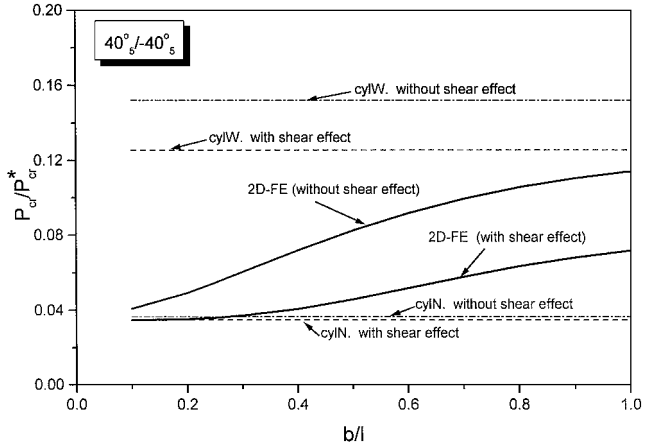

Fig. 4 Buckling load vs width-to-length ratio, $0 < b/l \leq 1$ for $40_5/-40_5$-deg laminate.

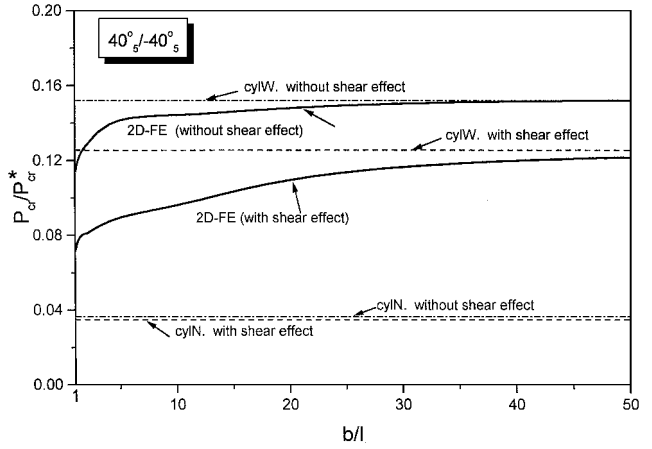

Fig. 5 Buckling load vs width-to-length ratio, $1 < b/l \leq 50$ for $40_5/-40_5$-deg laminate.

results are seen to tend to the lower bound in Fig. 4 and to the upper bound in Fig. 5.

The significant difference between the results with and without shear deformation effect is due to the low $l/h(=10)$ ratio and the high $E_{11}/G_{13}(=140)$ ratio, but the same conclusion applies to the constitutive models.

Conclusion

The well-known plane-strain and plane-stress constitutive models are unsuitable for composite laminated one-way panels. Cylindrical bending models are much more accurate and appropriate for presentation of laminated stacking combinations and orientations.

Acknowledgments

This study was partially supported by the fund for the promotion of research at the Technion. The authors are indebted to E. Goldberg for editorial assistance.

References

[1]Whitney, J. M., "Cylindrical Bending of Unsymmetrically Laminated Plates," *Journal of Composite Materials*, Vol. 3, 1969, pp. 715–719.

[2]Whitney, J. M., *Structural Analysis of Laminated Anisotropic Plates*, Technomic, Lancaster, PA, 1987, pp. 69–85.

[3]Sheinman, I., "Cylindrical Buckling Load of Laminated Columns," *Engineering Mechanics*, Vol. 115, No. 3, 1989, pp. 659–661.

[4]Sheinman, I., and Karadomateas, G. A., "Energy Release Rate and Stress Intensity Factors for Delaminated Composite Laminates," *International Journal of Solids Structures*, Vol. 34, No. 3, 1997, pp. 451–459.

[5]"COSMOS7," Structural Research and Analysis Corp., Santa Monica, CA, 1984.

A. M. Waas
Associate Editor

Failure Analysis of Scarf-Patch-Repaired Carbon Fiber/Epoxy Laminates Under Compression

C. Soutis* and F. Z. Hu†
Imperial College of Science, Technology, and Medicine, London, England SW7 2BY, United Kingdom

Introduction

In recent years, demands on technological development for permanent field and depot repairs of composite structures have increased considerably. As a result, repair methodologies have been developed and include a wide range of approaches, from highly refined and structurally efficient but expensive flush-patch repairs to mechanically attached metal-patch[1–3] repairs. Flush, scarf-type, bonded repairs are used on critical, highly loaded components, where load concentration and eccentricities, especially for compressive loading, must be avoided.[2]

Design methods for adhesively bonded repairs require criteria to predict both strength and durability. In this study, a three-dimensional stress analysis is performed to determine the stresses in a flush-scarf-repaired laminate under uniaxial compression (Fig. 1) so that predictions can be made of the optimum scarf angle and likely points of failure.

Scarf Joint and Optimum Scarf Angle

The joint of interest has identical adherends, uses a relatively brittle adhesive, and has small scarf angles (Fig. 2). For this simple case, the semiempirical analysis[4] predicts that the optimum scarf angle for a maximum strength joint is a function of the adhesive shear strength τ_s and laminate strength σ_{un}, given by

$$\theta_{opt} \cong \tan^{-1}(0.816\tau_s/\sigma_{un}) \tag{1}$$

For small θ, the failure stress $S_{g,f}$ of the scarf joint is determined by the maximum stress failure criterion,

$$S_{g,f} = \sigma_{un}/K_L = \tau_s/(K_A \sin\theta) \tag{2}$$

Received 10 July 1998; revision received 2 November 1999; accepted for publication 9 December 1999.

*Reader in Mechanics of Composites, Department of Aeronautics.
†Research Associate, Department of Aeronautics.

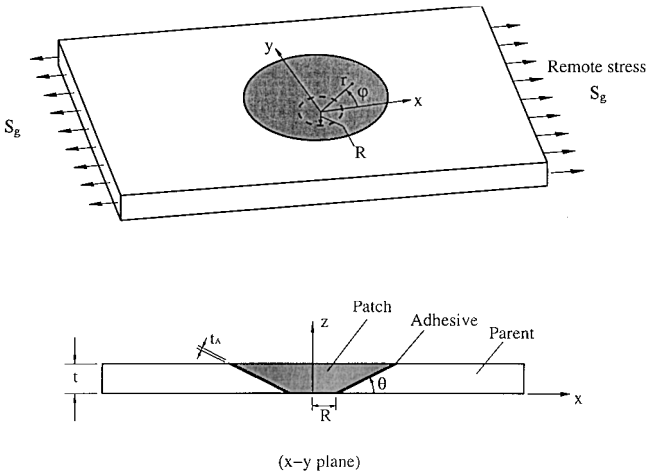

Fig. 1 Specimen geometry of the flush-scarf-type bonded repair (length = 304.8 mm, width = 152.4 mm, R = 25.4 mm, t = 2.27 mm, and t_A = 0.129 mm).

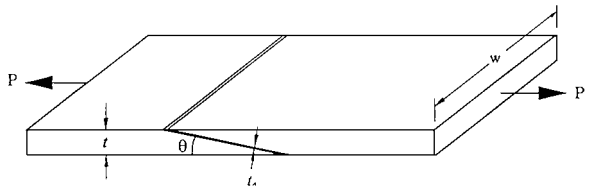

Fig. 2 Schematic of the scarf-joint geometry.

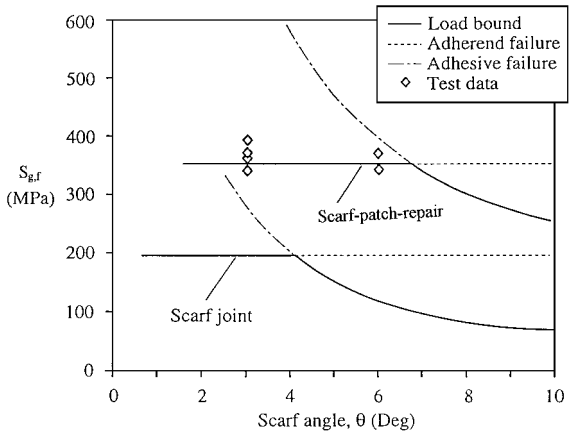

Fig. 3 Failure stress vs scarf angle for the scarf joint and the scarf-patch-repaired laminate. A characteristic length d_0 = 1 mm is used to correlate the test data.[5]

where K_A and K_L are the stress concentration factors (SCFs) in the adhesive and adherend, respectively. Based on the correlation with experimental data,[4,5] $K_A = 2.88$ and $K_L \approx 2.35$, for $\theta \leq 10$ deg. The load-carrying capabilities of the adhesive and the adherends in the joint are plotted in Fig. 3 as a function of scarf angle. The optimum scarf angle occurs when the adhesive failure load is equal to the laminate failure load. For the composite system examined ($\tau_s = 40$ MPa and $\sigma_{un} = 454$ MPa), Eq. (2) results in $\theta_{opt} = 4$ deg and a failure stress ≈ 200 MPa, which is more than 40% lower than the value measured for the scarf-patch repair shown in Fig. 1.

Flush Scarf-Patch Repair

Elastic Finite Element Analysis

The scarf-patch-repaired laminate (Fig. 1) is generally a three-dimensional problem, which is oversimplified by the scarf joint model described earlier. In a scarf joint, all loads are transferred through the adhesively bonded interface. In fact, the parent plate can still carry load after losing the support of the patch (a plate with a tapered open hole). Therefore, a three-dimensional stress analysis together with an appropriate failure criterion should be performed.

The FE-77 finite element package[6] is used to determine the three-dimensional stress field in the repaired laminate, using an isoparametric eight-node solid element. Because of the symmetry of the loading and hole location, only one-quarter of the plate is modeled. Because a high stress concentration is expected near the bonded interface, a fine mesh refinement is required in this area. The smallest element size in the radial direction is 0.0125 mm. The Celion/LARC-160 composite laminate and the patch, $[\pm 45/0/90]_{2s}$, are treated as homogeneous, elastic materials with the same properties[5]: $E_{xx} = E_{yy} = 53.8$ GPa, $E_{zz} = 11.3$ GPa, $G_{xy} = 20.5$ GPa, $G_{xz} = G_{yz} = 4.85$ GPa, $\nu_{xy} = 0.31$, $\nu_{xz} = \nu_{yz} = 0.19$, and compressive strength $\sigma_{un} = 454$ MPa. The epoxy adhesive layer of thickness $t_A = 0.129$ mm has the following stiffness and strength properties[5]: $E = 3.40$ GPa, $G = 1.26$ GPa, $\nu = 0.35$, and $\tau_s = 40$ MPa.

Stress Results

It is found that the dominant stress components are the in-plane stress σ_x in the parent laminate and the shear stress τ tangent to the tapered bond surface. The stress contours in the parent plate, patch, and adhesive layer are plotted for a scarf angle of 3 deg in Fig. 4. Other in-plane and through-thickness stress components are relatively small and could be neglected in the failure load calculations. A significant σ_x stress concentration occurs at the scarf tip of the parent plate and the patch, as shown in Fig. 4a. The patch is subjected to relatively low stresses, as shown in Fig. 4b, and the shear stress in the adhesive is quite uniformly distributed in the radial direction, as shown in Fig. 4c. The predicted peak stress positions coincide with those observed experimentally.[5]

The axial stress distribution σ_x along the x axis (load axis) has a steep gradient near the tip of the scarf ($x = R$, $y = 0$), suggesting the existence of stress singularity, and approaches the applied remote stress S_g within eight plies (1 mm). Because a mathematical stress singularity exists at the scarf tip as a result of stiffness discontinuity, the computed stresses are taken near but not at the tip of the scarf (Fig. 5). The stresses closest to the scarf tip are at $r - R = 0.5$ h; that is, at a distance of 0.0625 mm. As the distance from the tip ($r - R$) increases, the in-plane stress σ_x rapidly decreases. The largest compressive stress concentration factor ($K_t = 1.7$) occurs at $\varphi = 0$ deg ($r - R = 0.5$ h, $y = 0$) and is reduced to 1.06 at $\varphi = 90$ deg (0, R), compared with 3.6 for the case with an open hole; σ_x shows no significant variation along the y axis. Figure 5 suggests that σ_x is large in the region -60 deg $\leq \varphi \leq 60$ deg at $r - R < 5$ h. The shear stress τ varies mainly in the circumferential direction; its maximum value occurs at $\varphi = 0$ deg along the x axis and becomes zero along the y axis. Its magnitude is nearly proportional to the scarf angle; for $\theta = 9$ deg, τ is almost three times higher than the value obtained for $\theta = 3$ deg.

Strength Prediction

The stress analysis given here has shown that the dominant stress components are σ_x and τ for the parent laminate and the adhesive layer, respectively. The maximum stress failure criterion, for $K_t = 1.7$ at distance $r - R = 0.5$ h and $\sigma_{un} = 454$ MPa, predicts a residual strength of 267 MPa, which is ~25% less than the measured value.[5] A SCF value taken at distance $r - R = 2$ h would produce a better agreement. This suggests that stress redistribution, caused by material nonlinearities, occurs in the repaired region before final failure, and that using an elastic SCF can substantially underestimate the failure load.

Previous work[7,8] has shown that the approach for predicting failure in such laminates is that of averaging the stresses over a distance from the tip of the scarf, suggesting that the exact values of the stresses at the tip are not too important. The average stress failure criterion (ASFC) assumes that failure occurs when the average stress over a length d_0 from the scarf tip equals the ultimate strength of the material. The average of the stress component σ_x is defined as

$$\bar{\sigma}_x = \frac{1}{d_0} \int_R^{R+d_0} \sigma_x \, dx \tag{3}$$

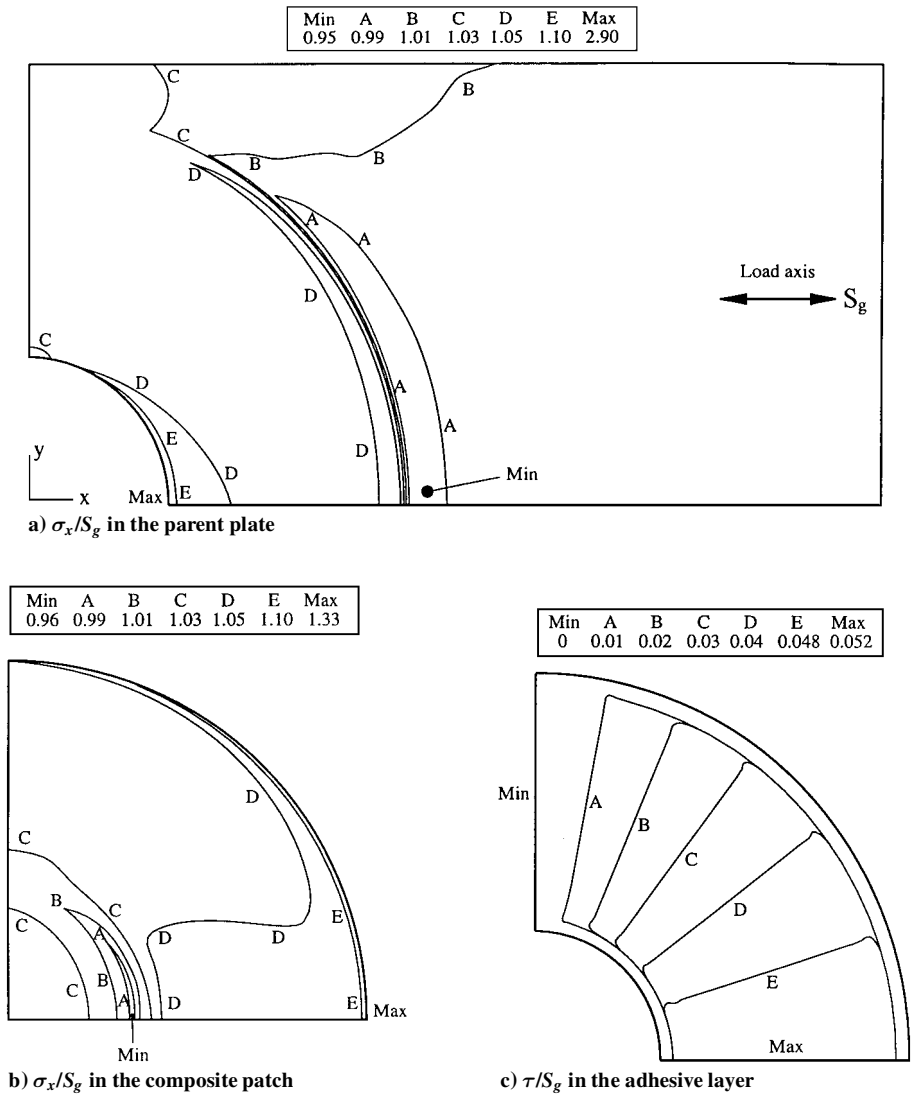

a) σ_x/S_g in the parent plate

b) σ_x/S_g in the composite patch

c) τ/S_g in the adhesive layer

Fig. 4 Finite element stress contours in the scarf-patch-repaired laminate.

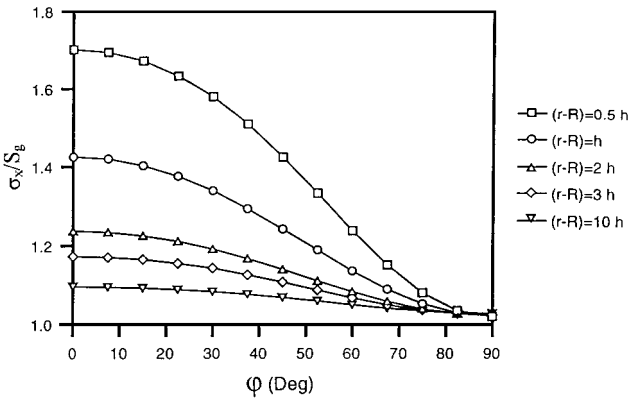

Fig. 5 Circumferential distributions of σ_x/S_g in the parent plate for $\theta = 3$ deg.

Failure in the parent laminate occurs when $\bar{\sigma}_x = \sigma_{un}$, and similarly in the adhesive when $\bar{\tau} = \tau_s$.

When a characteristic length $d_0 = 1$ mm is assumed, the failure load of the scarf-patch repair is obtained as a function of the scarf angle, Fig. 3; for the composite system examined, the optimum scarf angle is almost 7 deg compared with 4 deg obtained by using Eq. (2) for the scarf joint. The experimental strength data[5] are in good agreement with the theoretical predictions. This is not surprising, because adjustable parameter d_0 is based on the correlation with experimental data; d_0 accounts for material nonlinearities and plasticity of the adhesive that reduce local peak stresses in the repaired region. These are stress redistribution mechanisms that are not considered in the elastic finite element analysis.

Conclusion

Simple analytical and numerical models were presented to determine the optimum geometry and compressive strength of flush composite repairs. To account for material nonlinearities and plastic deformation of the adhesive, the ASFC is used with the finite element stress distributions to estimate the ultimate strength of the three-dimensional repaired configuration. This avoids the need for a nonlinear analysis, thus saving on computation time and memory requirements. The simple scarf-joint analysis underestimates the strength of the scarf patch repair by more than 40% and predicts an optimum scarf angle of 4 deg compared with an angle of almost 7 deg obtained by the ASFC. A 4-deg scarf angle would remove too much undamaged material and weaken the repaired laminate. Adding a safety factor to this value to account for temperature effects, manufacturing anomalies, fatigue, and endurance life would reduce θ from 4 deg probably down to 1–2 deg, which is extremely difficult to manufacture.

Acknowledgment

The authors are grateful for funding from the British Engineering and Physical Sciences Research Council (GR/K54892).

References

[1]Matthews, F. L. (ed.), *Joining Fibre-Reinforced Plastics*, Elsevier, New York, 1987.

[2]Hart-Smith, L. J., "Adhesive-Bonded Scarf and Stepped-Lap Joints," NASA CR-112237, Jan. 1973.

[3]Soutis C., and Hu, F. Z., "Design and Performance of Bonded Patch Repairs of Composite Structures," *Proceedings of the Institute of Mechanical Engineers*, Vol. 211, Pt. G, 1997, pp. 263–271.

[4]*Advanced Composite Design Guide*, Vol. 2, *Analysis*, 3rd ed., U.S. Air Force Materials Lab., Wright–Patterson AFB, Dayton, OH, Jan. 1973.

[5]Jones, J. S., and Graves, S. R., "Repair Techniques for Celion/LARC-160 Graphite/Polyimide Composite Structures," NASA CR-3794, June 1984.

[6]Hitchings, D., *Finite Element Package FE-77 User's Manual*, Imperial College, London, 1995.

[7]Hu, F. Z., Soutis, C., and Edge, E. C., "Interlaminar Stresses in Composite Laminates with a Circular Hole," *Composite Structures*, Vol. 37, No. 3, 1997 pp. 223–232.

[8]Soutis, C., and Hu, F. Z., "Repair Design of Composites and Efficiency of Scarf Patch Repairs," *Proceedings of the ICCM*, edited by M. L. Scott, Vol. 11, Woodhead Publishing Ltd., Gold Coast, Australia, 1997, pp. 395–404.

G. A. Kardomateas
Associate Editor